Published in final edited form as:
Biochem J. 2010 September 1; 430(2): 285–293. doi:10.1042/BJ20091378.

Mammalian thioredoxin reductase 1: roles in redox homoeostasis and characterization of cellular targets

Anton A. Turanov[*,†,1], **Sebastian Kehr**[*,1,2], **Stefano M. Marino**[*,†], **Min-Hyuk Yoo**[‡], **Bradley A. Carlson**[‡], **Dolph L. Hatfield**[‡], and **Vadim N. Gladyshev**[*,†,3]

[*]Department of Biochemistry and Redox Biology Center, University of Nebraska, Lincoln, NE 68588, U.S.A

[†]Division of Genetics, Department of Medicine, Brigham & Women's Hospital and Harvard Medical School, Boston, MA 02115, U.S.A

[‡]Molecular Biology of Selenium Section, Laboratory of Cancer Prevention, Center for Cancer Research, National Cancer Institute, National Institutes of Health, Bethesda, MD 20892, U.S.A

Abstract

The classical Trx (thioredoxin) system, composed of TR (Trx reductase), Trx and NADPH, defines a major pathway of cellular thiol-based redox regulation. Three TRs have been identified in mammals: (i) cytosolic TR1, (ii) mitochondrial TR3 and (iii) testes-specific TGR (Trx-glutathione reductase). All three are selenocysteine-containing enzymes with broad substrate specificity in *in vitro* assays, but which protein substrates are targeted by TRs *in vivo* is not well understood. In the present study, we used a mechanism-based approach to characterize the molecular targets of TR1. Cytosolic Trx1 was the major target identified in rat and mouse liver, as well as in rat brain and mouse serum. The results suggest that the main function of TR1 is to reduce Trx1. We also found that TR1-based affinity resins provide a convenient tool for specific isolation of Trxs from a variety of biological samples. To better assess the role of TRs in redox homoeostasis, we comparatively analysed TR1- and TR3-knockdown cells. Although cells deficient in TR1 were particularly sensitive to diamide, TR3-knockdown cells were more sensitive to hydrogen peroxide. To further examine the TR1–Trx1 redox pair, we used mice with a liver-specific knockout of selenocysteine tRNA. In this model, selenocysteine insertion into TR1 was blocked, but the truncated form of this protein was not detected. Instead, TR1 and TR3 levels were decreased in the knockout samples. Diminished hepatic TR1 function was associated with elevated Trx1 levels, but this protein was mostly in the oxidized state. Overall, this study provides evidence for the key role of the TR1–Trx1 pair in redox homoeostasis.

Keywords

cellular target; redox control; thioredoxin; thioredoxin reductase 1

[3]To whom correspondence should be addressed (vgladyshev@rics.bwh.harvard.edu).
[1]These authors contributed equally to the present study.
[2]Present address: Interdisciplinary Research Center (IFZ), Justus-Liebig University Giessen, Heinrich-Buff-Ring 26-32, 35392 Giessen, Germany

AUTHOR CONTRIBUTIONS

Anton Turanov, Sebastian Kehr, Stefano Marino, Min-Hyuk Yoo and Bradley Carlson carried out experiments. Anton Turanov, Sebastian Kehr, Dolph Hatfield and Vadim Gladyshev wrote the manuscript and all authors contributed to the final revision of the manuscript.

INTRODUCTION

The Trx (thioredoxin) system is a key player in redox homoeostasis in mammals, along with the GSH system. The Trx system is composed of TR (Trx reductase) and Trx. Mammalian TRs are NADPH-dependent, FAD-containing enzymes [1–4]. They belong to a family of pyridine nucleotide-disulfide oxido-reductases, which also includes lipoamide dehydrogenase, NADH peroxidase, glutathione reductase and several other enzymes. Mammalian TRs are characterized by the presence of the C-terminal redox-active motif Gly-Cys-Sec-Gly, in which selenocysteine (Sec) is essential for the catalytic function of these enzymes [5].

Three TRs have been identified in mammals: (i) cytosolic TR1 (also known as TrxR1 or Txnrd1) [1], (ii) mitochondrial TR3 (also known as TrxR2 or Txnrd2) [6,7] and (iii) TGR (Trx-glutathione reductase; also known as TR2 or Txnrd3) which contains an additional N-terminal Grx (glutaredoxin) domain [8,9]. TR1 and TR3 are ubiquitously expressed in various tissues and cell types, whereas TGR occurs in very low levels in various tissues, except for testes, where TGR transiently accumulates in spermatids [9]. Mammalian cells contain two ubiquitously expressed Trxs. Trx1 is a cytosolic and nuclear protein, whereas Trx2 is targeted to mitochondria [10]. Cytosolic and mitochondrial Trx systems are essential for embryogenesis in mice, as deletion of any of their components (i.e. TR1, TR3, Trx1 or Trx2) leads to embryonic lethality [11–14]. The observation of an overall proliferation block in TR1-knockout mice supports the idea that TR1 is a major player in the cell proliferation machinery.

TRs are best known for their ability to reduce oxidized Trxs as part of the Trx system, but they exhibit a broad substrate spectrum in *in vitro* assays [2,3,7]. It is believed that their flexible C-terminal tail, which transfers electrons from the buried N-terminal redox-active site to a more solvent-exposed position, enables this broad range of substrates [2]. Additional substrates can be small non-protein molecules, such as dehydroascorbate, selenodiglutathione, *S*-nitrosoglutathione, ubiquinone, selenite and selenocystine, as well as proteins, such as NK-lysin, cytochrome *c*, protein-disulfide isomerase, glutathione peroxidases and many other proteins [2,3,15]. However, the physiological relevance of many of these substrates is unclear [15].

In order to identify molecular targets of TR1 intracellularly, we used a mechanism-based method to search for the TR1 substrates in rodents (Supplementary Figure S1 at http://www.BiochemJ.org/bj/430/bj4300285add.htm). These proteins were trapped on affinity columns containing immobilized TR1 forms and identified by Western blot analysis and MS/MS (tandem MS). Trx1 was found to be the major target of TR1 in all tissues examined. In fact, besides Trx, no other abundant protein was specifically enriched in the eluates from the TR affinity columns. Moreover, Trx1 could be efficiently isolated from mouse serum, even though it occurs there in extremely low levels. Therefore TR1 columns provide a convenient tool for specific enrichment of Trx1 from biological samples. We also found that deficiency in TRs led to elevated Trx1 expression, although this protein was in the oxidized state. Overall, the results of the present study show a key role of the TR1–Trx1 pair in redox regulation.

EXPERIMENTAL

Materials

EDTA, NADPH, sodium selenite, Tris/HCl, Hepes, DTT (dithiothreitol) and diamide were from Sigma, protease inhibitor cocktail (EDTA-free) was from Roche Applied Science, and LB (Luria–Bertani) and LB-agar medium powder was from QBioGene or MP Bio. Anti-

rabbit HRP (horseradish peroxidase)-coupled antibodies and ECL (enhanced chemiluminescence) detection reagents were from GE Healthcare. DMEM (Dulbecco's modified Eagle's medium), newborn calf serum, penicillin/streptomycin, Trypsin-EDTA solution, hygromycin B, AMS (4-acetamido-4′-maleimidylstilbene-2,2′-disulfonic acid), Lipofectamine™ 2000 and Plus reagent were from Invitrogen. All antibodies used in the present study were developed in our laboratories [7], unless the source is indicated.

Cloning and expression of recombinant hTR1 (human TR1)

The following hTR1 (GenBank® accession number BC018122, corresponding to the major isoform of TR1) constructs were cloned into the pET28(a)+ vector: (i) WT (wild-type) enzyme (C-terminal sequence GCUG) with the *Escherichia coli* FdhH SECIS element; (ii) cysteine mutant (C-terminal sequence GCCG); (iii) cysteine-to-serine and selenocysteine-to-cysteine mutant (C-terminal sequence GSCG); (iv) selenocysteine-to-serine mutant (C-terminal sequence GCSG); (v) cysteine-to-serine and selenocysteine-to-serine mutant (C-terminal sequence GSSG); and (vi) truncated form (C-terminal sequence GC). These constructs were expressed in *E. coli* BL21 (Novagen) cells. To express the selenocysteine-containing TR1, cells were co-transformed with the pSUABC plasmid (kindly provided by Dr Elias Arnér, Karolinska Institute, Stockholm, Sweden; [16]). Protein expression was induced by adding 0.5 mM IPTG (isopropyl β-D-thiogalactoside) when the cells reached an A_{600} of ~ 0.6. Sodium selenite was added to a final concentration of 2 μM approx. 1 h prior to induction of protein synthesis. After induction, the cells were grown overnight at 30 °C, harvested by centrifugation (6000 ***g*** for 20 min at 4 °C) and stored at −80 °C. After purification of the His-tagged proteins on Ni–Sepharose columns, the purity of proteins was determined by SDS/PAGE. Fractions containing TR1 were combined, dialysed against PBS, concentrated and stored at −80 °C. The protein concentrations were determined using the Bradford assay (Bio-Rad).

Preparation of hTR1-immobilized resins and target search

Recombinant TR1 forms were used to prepare Sepharose-based affinity columns as described previously for mTR3 (mouse TR3) [7] and in the Supplementary material (at http://www.BiochemJ.org/bj/430/bj4300285add.htm). Typically, more than 90 % of the applied recombinant TR1 could be immobilized. In order to search for targets, the immobilized enzymes were initially reduced with 2 ml of 0.5 mM NADPH and 50 mM Tris/HCl (pH 8.0), for 20 min. Various tissue homogenates (15–30 mg) (Supplementary material) and body fluids were applied to each column. After 1 h of incubation at room temperature (22 °C) with end-over shaking, the resins were washed five times with 50 mM Tris/HCl (pH 8.0) and 300 mM NaCl, to remove non-specifically bound proteins. Finally, proteins were eluted with 800 μl of 50 mM Tris/HCl (pH 8.0), 300 mM NaCl and 10 mM DTT. The proteins were separated by SDS/PAGE and the gels were stained with Coomassie Blue or a silver staining solution (Bio-Rad or Pierce). Protein bands of interest were cut from the gels, subjected to trypsin digestion, and protein sequences were determined by MS/MS at the Nebraska Redox Biology Center MS facility. Western blots were carried out with Trx1 antibodies [7] and the membranes were also stained with Coomassie Blue.

Silencing mTR3 expression in NIH 3T3 cells

The Silencer Express siRNA Expression Cassette Kit (Ambion) was used to generate a siRNA (small interfering RNA) expression vector to knockdown TR3 in NIH 3T3 cells. The siRNA target sequences were chosen using siRNA Design (http://www.ambion.com/techlib/misc/siRNA_finder.html). Cells were separately transfected with five constructs (four siRNA targets and one for negative control, pSEC hygro). NIH 3T3 cells were grown in DMEM supplemented with 10 %FBS (fetal bovine serum) and 1 × solution (Invitrogen)

antibiotic/antimycotic solution at 37 °C. Stably transfected siTR3 and pSEC hygro cells were prepared by transfecting with the corresponding constructs using Lipofectamine™ 2000 and Plus reagent and selecting cells in the presence of 500–1000 μg/m hygromycin B. Protein expression was examined by Western blot analysis using anti-mTR3 and anti-mTR1 antibodies. Two siTR3 constructs (siTR3 1.1 and siTR3 1.3) were particularly efficient in TR3 knockdown, and the corresponding stably transected cell lines were used in further experiments.

Analysis of sensitivity of TR3- and TR1-knockdown cells to oxidative stress

TR3-knockdown cells were tested for their sensitivity to oxidative stress caused by hydrogen peroxide, diamide or menadione treatments. In total, 5×10^3 cells per well were seeded in 96-well plates and grown overnight in DMEM containing 10 % FBS. Cells were washed twice with PBS, the medium was replaced with serum/phenol-red-free medium and cells were treated with various concentrations of oxidants for 1 h. Alternatively, cells in PBS were irradiated by UV (254 nm, 40 J/m^2), PBS was replaced with DMEM containing 10 % FBS, and cells were maintained for 6 or 12 h at 37 °C. Cell viability and growth were determined using a CellTiter 96 AQeus One Solution Cell Proliferation Assay Kit (Promega). The siTR1-knockdown TSMK-1 cell line was maintained as described previously [17] and treated with hydrogen peroxide and diamide as described above for TR3-knockdown cells.

Metabolic labelling of selenoproteins with ^{75}Se

Mice with genotypes *Trspfl/fll-Alb-Cre*+/− (+/−), *Trspfl/+-Alb-Cre*+/− (−/ −) and *Trspfl/fll* (WT) were injected intraperitoneally with 50 μCi of ^{75}Se/g of body weight and killed 48 h after injection. Tissues and organs were excised, immediately placed in liquid nitrogen and stored until use [18]. Liver lysates were loaded on to ADP–Sepharose resins, the resins extensively washed with loading buffer and bound proteins were eluted with SDS/PAGE loading buffer. Isolated proteins were subjected to SDS/PAGE followed by Western blotting with antibodies specific for TR1, TR3, Trx1 and Trx2 [7]. ^{75}Se-labelled proteins were detected with a PhosphorImager. Western blot images were quantified using ImageQuant and the results represented as means ± S.D. for three independent experiments in which the values for WT samples were normalized to 100 %.

Animal experimentation was carried out according to the legal requirements of the Association for Assessment and Accreditation of Laboratory Animal Care International and the Institutional Care and Use Committee of the University of Nebraska (Lincoln, NE, U.S.A.).

Analysis of the redox state of Trx in selenocysteine tRNA gene (Trsp) knockout mice

To determine the redox state of Trx, liver lysates were treated with AMS, a compound that alkylates reduced cysteine residues. Alkylation of cysteine residues decreases mobility of the modified proteins on SDS gels. Briefly, ice-cold TCA [trichloroacetic acid; 15 % (v/v)] was added to samples, and they were incubated on ice for 15 min. Precipitated proteins were centrifuged at 2000 ***g*** for 10 min, washed with ice-cold acetone and recentrifuged. The samples were dried and proteins resuspended in 20 μl of 100 mM sodium phosphate (pH 7.0), 1 mM EDTA and 1 % SDS. Then, 15 mM AMS was added. Alkylation was performed at 37 °C for 2 h. Control samples were incubated with 10 mM diamide or 10 mM DTT for 30 min prior to AMS treatment of oxidized and reduced Trx controls respectively. Proteins were subjected to SDS/PAGE under non-reducing conditions, followed by Western blot analysis with anti-Trx1 antibodies.

Docking of TR1 and Trx1

The rat TR1 structure (PDB code 3EAN) was downloaded from the PDB (http://www.rcsb.org/pdb/explore/explore.do?structureId=3EAN). For consistency, rat Trx1 (*>gi|149037133*) was used as a docking partner. The protein was modelled with Swiss Model (http://swissmodel.expasy.org/), based on the highly similar (sequence identity 86 %) human protein (PDB code 1TRS, oxidized form). Docking calculations were made with two programs: standalone Hex 5.0 (http://www.csd.abdn.ac.uk/hex/) and the RosettaDock web server (http://rosettadock.graylab.jhu.edu/). In each case, it was necessary to prepare an *in silico* model of the U498C mutant TR1 structure, as the force-field employed did not recognize and properly treat selenocysteine residues (see the Supplementary Experimental section at http://www.BiochemJ.org/bj/430/bj4300285add.htm).

RESULTS AND DISCUSSION

Preparation of recombinant TR1 forms and TR1-based affinity columns

We employed a mechanism-based chromatographic approach to identify cellular targets of TR1. Reduction of any protein substrate by TR1 involves formation of an intermediate intermolecular selenenylsufide (or disulfide) bond which is formed when the reduced C-terminal active site of TR1 attacks the oxidized active site in the substrate. This intermediate is then resolved to generate an oxidized selenenylsulfide within TR1 and a reduced dithiol within the target. To trap intermolecular intermediates between TR1 and its targets, we removed a resolving residue in TR1, leaving only a single cysteine or selenocysteine residue in the C-terminal active site (Supplementary Figure S1 at http://www.BiochemJ.org/bj/430/bj4300285add.htm). We generated several recombinant hTR1 forms to trap TR1 targets in the intermediate step, including: (i) WT protein with the C-terminal GCUG sequence (designated CU for Cys–Sec pair; owing to inefficient selenocysteine insertion, this protein is a mixture of WT and truncated forms); (ii) form in which cysteine replaced selenocysteine (CC for Cys–Cys pair); (iii) form in which serine replaced cysteine, and cysteine replaced selenocysteine (SC for Ser–Cys pair); (iv) form in which cysteine and selenocysteine were replaced with serine (SS for Ser–Ser pair); and (v) truncated form in which the selenocysteine UGA codon served as stop (C for cysteine-truncated mutant) (Figure 1 and Supplementary Figure S1). For the expression of the selenocysteine-containing form, the construct was designed to contain a bacterial SECIS element downstream of the selenocysteine codon, and this construct was co-expressed with a plasmid coding for three genes of the bacterial selenocysteine insertion machinery [16]. Purified recombinant TR1 forms were then immobilized to generate TR1-based affinity columns or resins as described in the Experimental section and the Supplementary material.

Identification of TR1 substrates

To identify TR1 target molecules, we initially investigated cytosolic fractions from mammalian liver, an organ that is characterized by high levels of Trx and GPx1 (glutathione peroxidase 1) expression (Supplementary Figure S2 at http://www.BiochemJ.org/bj/430/bj4300285add.htm) [2]. Mouse and rat liver cytosolic fractions were incubated with TR1-affinity resins. Four of the affinity resins were used as controls: (i) the Ser–Ser TR1 form was the principal negative control as it lacks the entire redox pair in the C-terminus, eliminating any chance for a possible redox interaction with a target molecule; (ii) Cys–Sec and (iii) Cys–Cys TR1 forms were negative controls because they possess both redox active residues of the redox pair in the C-terminus, which should resolve most intermediate enzyme–target complexes; and (iv) the C-truncated TR1 form was used as a positive control as it has just one redox-active residue of the redox pair in the C-terminus (no resolving cysteine residue) and its model is more likely to bind to TR1 targets when compared with the WT enzyme. After incubation with the tissue homogenate, the TR1-affinity resins were

washed extensively to remove non-specifically bound proteins. Trapped proteins were eluted with a buffer containing the reductant DTT. Analysis of the elution fractions using SDS/PAGE revealed several protein bands in the Coomassie-Blue-stained gel, independent of the TR1-affinity column used (Figure 1). There are four potential reasons for the interaction of proteins with the column: (i) binding of proteins to TR1 irrespective of the redox state, (ii) specific redox binding, (iii) non-specific redox interaction, and (iv) non-specific, non-redox interaction. Thus the proteins that occurred in the elution fractions independent of the TR1 form used were considered to be non-specific or non-redox TR1 targets and were not further analysed. A 12 kDa band was clearly enriched in the fractions eluted from the columns containing cysteine–selenocysteine, serine–cysteine and C-truncated forms of TR1. This band was less abundant in the case of cysteine–cysteine fractions and was essentially missing in the fraction eluted from the serine–serine TR1 resin (Figure 1). The enrichment of the 12 kDa band in the case of the WT TR1 was due to the presence of the truncated form of this enzyme, because selenocysteine insertion in bacteria is inefficient, even when cells are co-transformed with the plasmid expressing components of the bacterial selenocysteine insertion machinery [7]. In addition, a 55 kDa band, which occurred in all elution fractions, probably corresponds to TR1, which was enriched because (i) TR1 could be partially released from the affinity resin by losing one of its subunits, and/or (ii) endogenous TR from the homogenate interacted with the resin-bound TR to form dimers and tetramers.

Trx1 is a 12 kDa protein and the best-known TR1 substrate, and therefore we carried out Trx1 Western blots. The trapped protein was indeed Trx1 as shown in the three lower panels in Figure 1. We also sequenced the band by MS/MS and only Trx1 was identified with an average sequence coverage of approx. 30 % (Supplementary Table S1 at http://www.BiochemJ.org/bj/430/bj4300285add.htm). Thus we conclude that cytosolic Trx1 is the major redox target of TR1 in mouse and rat liver. Although Trx1 must be in the oxidized state to interact with TR1, preparation of lysates in air led to a partial oxidation of proteins. Control experiments confirmed specificity of Trx1 coupling to NADPH-reduced TR1 columns, whereas untreated or hydrogen-peroxide-oxidized TR1 showed insignificant Trx binding with concomitant increase of non-specifically bound proteins (Supplementary Figure S2B).

To search for additional TR1 targets, we examined tissues with lower Trx1 expression (1–10 μM Trx) to decrease the competition between Trx1 and low abundance targets for TR1 binding. We analysed rat brain and mouse serum. In this experiment, we only used an affinity resin with the C-truncated form of TR1 as the most effective one in trapping TR1 targets and the serine-serine TR1 form column as a control. Again, the only specific TR1 target band isolated from rat brain and mouse serum migrated as a 12 kDa protein and was identified as Trx1 by Western blot analysis and peptide sequencing (Figure 1C, lower panel and Supplementary Table S1). This is especially intriguing for mouse serum, in which the Trx1 levels are extremely low (1–10 nM) [2]. Although Trx1 is secreted as full-length and truncated forms [19,20], we only detected the full-length form, suggesting that the truncated Trx1 form is either much less abundant or it is not trapped by the TR1 column. A 55 kDa band was also observed in the rat brain sample that corresponds to TR1 (see above). All other bands eluted equally from cysteine and serine–serine columns and were considered to be non-specific or non-redox TR1 targets.

With our affinity column approach we identified Trx1 as the major target of TR1 in all samples analysed, including liver, brain and serum. Because it might be that the targets with extremely low abundance could not be identified by our method, our conclusion holds only for relatively abundant proteins and, among these proteins, only Trx1 is the mechanism-based substrate. Moreover, abundant Trx1 bands were observed following a single-step procedure from crude extracts of liver and brain (Supplementary Figure S3 at http://

www.BiochemJ.org/bj/430/bj4300285add.htm). Thus this method can be used for further searches of TR targets in other cellular compartments, such as the endoplasmic reticulum and mitochondria. We suggest that this mechanism-based affinity approach will be useful for isolation of Trxs from a variety of biological samples for further analyses, e.g. post-translational modifications and binding partners. The method may also be applied to certain other pyridine nucleotide disulfide oxidoreductases.

Interaction of the C-terminal region of TR1 with Trx1

Recently, a structure of rat TR1, including its C-terminal region, was reported [21]. We took advantage of this work to investigate the interaction between TR1 and Trx1 by protein–protein docking (Figure 2). In our calculations, we consistently found only one binding mode. Specifically, Trx1 docked to the region of TR1 delimitated by its C-terminal coil and the third helix (spanning residues Trp^{98} to Lys^{123}). Through this interaction, the catalytic Cys^{32} of Trx1 gets closer to Cys^{497} and away from Sec^{498}. Thus a possibility that Cys^{497}(TR1)–Cys^{32}(Trx1) is the interacting cysteine pair in the catalytic process of Trx1 reduction, whereas Sec^{498} serves as a resolving residue, cannot be excluded. Our model is comparable with the recent model of the TR1–Trx1 complex [21], but it represents the first docking simulations of TR1–Trx1 interaction.

Analysis of the docking structure showed that the C-terminal coil region of TR1 was somewhat lodged in a helical region (Figure 2, right-hand side). In this predicted position, the C-terminal Sec^{498}–Gly^{499} residues face the upcoming Trx1 from opposite positions. Thus with the docking trajectory shown in the Figure, even if Sec^{498} is accessible to the solvent, its reactive functional group is exposed in the opposite direction with respect to Trx1 direction. Not considering rearrangements in the TR1 structure (based on PDB code 3EAN, reduced form), a model wherein selenocysteine is the nucleophilic-attacking group would require Trx1 to approach and dock closer to helix 1 (i.e. docking from the left-hand side in the Figure), thus requiring a different trajectory. In our calculations, we did not observe such an alternative approach. However, even if, in our best scoring calculations, Cys^{497} directly pointed to the catalytic site of Trx1, it was at ~ 5.8 Å (1 Å = 0.1 nm) (a weighted value given the imprecision at the atomic level of protein–protein docking), still quite far from Cys^{497}. Therefore it is likely that the mobile C-terminus of TR1 has to move forward, shifting laterally to α-helix 3 and moving away from Leu^{112}, Gly^{115} and Ala^{119} (the closest residues to Cys^{497}, all belonging to α-helix 3) in the direction of Trx1. In this regard, the truncated form of TR1 may have advantage in interacting with Trx1: although the full-size protein needs to overcome steric resistance (i.e. undergoing heavier local rearrangements) to let their mobile C-terminal region approach the Trx1 active site, the truncated form could more easily approach and interact with the catalytic Cys^{32}.

Sensitivity of TR1-knockdown cells to oxidative stress

Previously established TCMK-1 TR1-knockdown cells showed increased sensitivity to UV irradiation [17]. Although these cells were characterized by ~ 90 % reduction in TR1 expression (Figure 3A), they had normal viability in the absence of stress. To better understand the role of TR1 in redox homoeostasis, we examined the sensitivity of these cells to various forms of oxidative stress. Interestingly, hydrogen peroxide had no effect, but these cells were sensitive to diamide (Figures 3B and 3C). The difference with the control was statistically significant at 100 μM ($P < 1 \times 10^{-6}$) and 200 μM ($P < 0.059$) diamide, and not statistically significant at a lower concentration, 50 μM ($P < 0.15$). It appears that, in the absence of TR1, diamide may cause rapid oxidation of Trx1 and its target proteins. However, other antioxidants, such as GPxs and catalase, may protect TR1-deficient cells from hydrogen peroxide.

Analysis of mTR3-knockdown cells

To compare TR1 and TR3 functions with respect to protection against oxidative stress, we established siRNA-based TR3-knockdown cell lines. We transfected NIH 3T3 cells with five constructs, four siRNA TR3 targets and one control, and isolated two clones (siTR3 1.1 and siTR3 1.3) that were characterized by a ~ 50 %reduction in TR3 expression (whereas TR1 expression was not affected in these cells) (Figure 4A). We observed a small decrease in the growth rate of these cells compared with the control cells (Figure 4B). The knockdown cells were further subjected to UV irradiation and showed an approx. 20 % decrease in cell viability (Figure 4C). TR3 and Trx2 may play a role in antioxidant defence [22,23]. Thus we subjected the TR3-knockdown cells to oxidative stresses caused by treatment with hydrogen peroxide, diamide and menadione (Figure 5). These cells were sensitive to hydrogen peroxide, especially at low concentrations, but not to menadione or diamide. The reduced growth rate of TR3-knockdown cells, as well as their sensitivity to hydrogen peroxide correlated with the reduction in TR3 expression. This is consistent with the findings that TR3 knockout in mice is associated with severe anaemia, increased apoptosis and death at embryonic day 13 [14]. Surprisingly, the effects of TR1 knockdown with regard to sensitivity to hydrogen peroxide and diamide were essentially opposite to that of TR3 knockdown. Thus our comparative analysis revealed differences in TR1 and TR3 function, which probably relates to their compartmentalization within mammalian cells. These studies further suggest an important role of these enzymes in redox regulation and protection against oxidative stress.

Analysis of TR expression in mice with liver-specific selenocysteine tRNA gene (*Trsp*) knockout

To further analyse the role of the Trx system in regulation of redox homoeostasis in mammals, we used mice with liver-specific knockout of *Trsp* [18]. In this model, lack of selenocysteine tRNA leads to the inability to synthesize selenoproteins in hepatocytes (Figure 6A). We carried out metabolic labelling of knockout mice with ^{75}Se to assess selenoprotein expression in comparison with that of control mice. To analyse TR1 and TR3 expression, liver extracts were applied to an ADP–Sepharose resin, which is known to enrich TRs and other pyridine nucleotide disulfide oxidoreductases. Initial flow-through and elution fractions were analysed by SDS/PAGE and PhosphorImager and, additionally, by Western blots with TR1 and TR3 antibodies. As expected, selenoprotein expression was dramatically reduced in selenocysteine tRNA-knockout mice, and this included TRs (Figure 6). Although the lower levels of ^{75}Se-labelled TRs were expected, the reduced levels of both TR1 and TR3, as assessed by Western blotting, were of interest and suggest the lack of truncated forms of TRs in the liver of selenocysteine tRNA-knockout mice. Thus, rather than reducing selenocysteine insertion into TRs and generating truncated proteins, selenocysteine tRNA-knockout hepatocytes lowered the expression of TRs (Figure 6B). A previous study found reduced levels of ^{75}Se-labelled TR1 and TR1 activity in liver-specific selenocysteine tRNA-knockout mice, yet normal levels of TR1 as analysed by Western blots [18]. However, the new data show no evidence of large amounts of truncated TR forms. The findings of reduced TR1 and TR3 levels and the lack of truncated forms were also consistent with the lack of Trx1- and Trx2-TR complex enrichment on ADP–Sepharose resins. Since truncated TRs lacking the last two residues are the most efficient TR forms for trapping Trx, these forms, if they exist, should have bound Trx and both proteins should have been enriched on ADP–Sepharose. However, Trx1 and Trx2 appeared exclusively in the flow-through fractions (Figure 6B).

Expression levels and redox state of Trx1 in mice with selenocysteine tRNA knockout in the liver

While assaying ADP–Sepharose-bound proteins, we observed that both Trx1 and Trx2 showed elevated levels in the samples from liver-specific selenocysteine tRNA-knockout mice (Figure 6B). We examined additional samples from these mice and again found elevated expression of both cytosolic and mitochondrial Trxs (Figure 7). These findings suggest that reduced expression of TRs lead to up-regulation of Trx expression, perhaps to partially compensate for loss of TR activity. To determine the general redox state of the cysteine residues in Trx in selenocysteine tRNA-knockout samples, we utilized AMS as an alkylating agent. This compound modifies reduced cysteine residues in proteins and is a widely used reagent to monitor cysteine oxidation. Cysteine modification with AMS adds ~ 0.5 kDa per cysteine residue and results in mobility shift of the protein on SDS/PAGE. AMS treatment of samples from WT, heterozygous and homozygous knockout mice revealed that the cysteine residues in Trx1 were mostly in the reduced state in WT mice, whereas in knockout mice the cysteine residues were mostly in the oxidized state. In a control experiment, WT samples were treated with diamide and DTT to oxidize and reduce respectively, cysteine residues prior to AMS treatment (Figure 8).

Conclusions

We employed a mechanism-based method to detect TR1 targets in biological samples and show that despite the broad substrate specificity of TRs, Trxs are their major cellular substrates. TR1-affinity columns, especially the resin with the immobilized truncated TR1 form, could efficiently enrich Trx1 from various tissue homogenates of rodents, even from samples with extremely low levels of this protein. This method may be useful for enrichment and characterization of Trxs in a variety of settings and systems, including the analysis of its redox state, binding partners, expression levels and post-translational modifications. Down-regulation of TR1 and TR3 expression by siRNA revealed that both enzymes were important for cell proliferation and protection against oxidative stress. However, TR1- and TR3-knockdown cells responded differently to hydrogen peroxide and diamide treatment, with TR1 contributing more to protection against diamide (probably protecting against global thiol oxidation) and TR3 against peroxide. To further analyse the functions and regulation of the TR1–Trx1 pair, we investigated mice with liver-specific disruption in the selenocysteine tRNA gene. Selenoprotein expression was decreased in the liver of knockout mice, and we also observed decreased ^{75}Se insertion into TR1. However, the truncated form of TR1 was not elevated, suggesting that mechanisms other than selenocysteine insertion regulate TR1 expression under conditions of selenocysteine tRNA deficiency. In addition, decreased TR1 levels were associated with an increased Trx1 expression; however, this protein was mostly in the oxidized state. It is possible that increased synthesis of Trx1 (which is synthesized as a reduced protein) can partially compensate for TR1 deficiency. Taken together, the results of the present study suggest that the major cellular targets of TRs are Trxs and, therefore, that they are key enzymes, which maintain the redox state of cysteine residues in proteins and regulate cellular redox homoeostasis.

Supplementary Material

Refer to Web version on PubMed Central for supplementary material.

Acknowledgments

FUNDING

This work was supported by the National Institutes of Health [grant number GM065204 (to V. N. G.)] and the Intramural Program of the Center for Cancer Research, NCl, NIH (to D. L. H.).

Abbreviations used

AMS	4-acetamido-4′-maleimidylstilbene-2,2′-disulfonic acid
DMEM	Dulbecco's modified Eagle's medium
DTT	dithiothreitol
FBS	fetal bovine serum
GPx	glutathione peroxidase
LB	Luria–Bertani
MS/MS	tandem MS
siRNA	small interfering RNA
TGR	thioredoxin-glutathione reductase
Trx	thioredoxin
TR	Trx reductase
hTR1	human TR1
mTR3	mouse TR3
WT	wild-type

References

1. Holmgren A, Bjornstedt M. Thioredoxin and thioredoxin reductase. Methods Enzymol. 1995; 252:199–208. [PubMed: 7476354]
2. Gromer S, Urig S, Becker K. The thioredoxin system: from science to clinic. Med Res Rev. 2004; 24:40–89. [PubMed: 14595672]
3. Mustacich D, Powis G. Thioredoxin reductase. Biochem J. 2000; 346:1–8. [PubMed: 10657232]
4. Arner ES. Focus on mammalian thioredoxin reductases: important selenoproteins with versatile function. Biochim Biophys Acta. 2009; 1790:495–526. [PubMed: 19364476]
5. Zhong L, Holmgren A. Essential role of selenium in the catalytic activities of mammalian thioredoxin reductase revealed by characterization of recombinant enzymes with selenocysteine mutations. J Biol Chem. 2000; 275:18121–18128. [PubMed: 10849437]
6. Lee SR, Kim JR, Kwon KS, Yoon HW, Levine RL, Ginsburg A, Rhee SG. Molecular cloning and characterization of a mitochondrial selenocysteine-containing thioredoxin reductase from rat liver. J Biol Chem. 1999; 274:4722–4734. [PubMed: 9988709]
7. Turanov AA, Su D, Gladyshev VN. Mouse mitochondrial thioredoxin reductase: characterization of alternative cytosolic forms and cellular targets. J Biol Chem. 2006; 281:22953–22963. [PubMed: 16774913]
8. Sun QA, Kirnarsky L, Sherman S, Gladyshev VN. Selenoprotein oxidoreductase with specificity for thioredoxin and glutathione systems. Proc Natl Acad Sci USA. 2001; 98:3673–3678. [PubMed: 11259642]
9. Su D, Novoselov SV, Sun QA, Moustafa ME, Zhou Y, Oko R, Hatfield DL, Gladyshev VN. Mammalian selenoprotein thioredoxin/glutathione reductase: Roles in disulfide bond formation and sperm maturation. J Biol Chem. 2005; 280:26491–26498. [PubMed: 15901730]
10. Arner ES, Holmgren A. Physiological functions of thioredoxin and thioredoxin reductase. Eur J Biochem. 2000; 267:6102–6109. [PubMed: 11012661]

11. Matsui M, Oshima M, Oshima H, Takaku K, Maruyama T, Yodoi J, Taketo MM. Early embryonic lethality caused by targeted disruption of the mouse thioredoxin gene. Dev Biol. 1996; 178:179–185. [PubMed: 8812119]
12. Nonn L, Williams RR, Erickson RP, Powis G. The absence of mitochondrial thioredoxin 2 causes massive apoptosis, exencephaly, and early embryonic lethality in homozygous mice. Mol Cell Biol. 2003; 23:916–922. [PubMed: 12529397]
13. Jakupoglu C, Przemeck GK, Schneider M, Moreno SG, Mayr N, Hatzopoulos AK, de Angelis MH, Wurst W, Bornkamm GW, Brielmeier M, Conrad M. Cytoplasmic thioredoxin reductase is essential for embryogenesis but dispensable for cardiac development. Mol Cell Biol. 2005; 25:1980–1988. [PubMed: 15713651]
14. Conrad M, Jakupoglu C, Moreno SG, Lippl S, Banjac A, Schneider M, Beck H, Hatzopoulos AK, Just U, Sinowatz F, et al. Essential role for mitochondrial thioredoxin reductase in hematopoiesis, heart development and heart function. Mol Cell Biol. 2004; 24:9414–9223. [PubMed: 15485910]
15. Holmgren, A. Selenoproteins in thioredoxin system. In: Hatfield, DL.; Berry, MJ.; Gladyshev, VN., editors. Selenium. Its Molecular Biology and Role in Human Health. 2. Springer; New York: 2006. p. 183-194.
16. Arner ES, Sarioglu H, Lottspeich F, Holmgren A, Böck A. High-level expression in *Escherichia coli* of selenocysteine-containing rat thioredoxin reductase utilizing gene fusions with engineered bacterial-type SECIS elements and co-expression with the selA, selB and selC genes. J Mol Biol. 1999; 292:1003–1016. [PubMed: 10512699]
17. Yoo MH, Xu XM, Turanov AA, Carlson BA, Gladyshev VN, Hatfield DL. A new strategy for assessing selenoprotein function: siRNA knockdown/knock-in targeting the 3′-UTR. RNA. 2007; 13:1–9. [PubMed: 17123956]
18. Carlson BA, Novoselov SV, Kumaraswamy E, Lee BJ, Anver MR, Gladyshev VN, Hatfield DL. Specific excision of the selenocysteine tRNA[Ser]Sec (Trsp) gene in mouse liver demonstrates an essential role of selenoproteins in liver function. J Biol Chem. 2004; 279:8011–8017. [PubMed: 14660662]
19. Okuyama H, Son A, Ahsan MK, Masutani H, Nakamura H, Yodoi J. Thioredoxin and thioredoxin binding protein 2 in the liver. IUBMB Life. 2008; 60:656–660. [PubMed: 18636507]
20. Nakamura H, Masutani H, Yodoi J. Extracellular thioredoxin and thioredoxin-binding protein 2 in control of cancer. Semin Cancer Biol. 2006; 16:444–451. [PubMed: 17095246]
21. Cheng Q, Sandalova T, Lindqvist Y, Arner ES. Crystal structure and catalysis of the selenocysteine thioredoxin reductase 1. J Biol Chem. 2009; 284:3998–4008. [PubMed: 19054767]
22. Patenaude A, Ven Murthy MR, Mirault ME. Mitochondrial thioredoxin system: effects of TrxR2 overexpression on redox balance, cell growth, and apoptosis. J Biol Chem. 2004; 279:27302–27314. [PubMed: 15082714]
23. Chen Y, Cai J, Jones DP. Mitochondrial thioredoxin in regulation of oxidant-induced cell death. FEBS Lett. 2006; 580:6596–6602. [PubMed: 17113580]

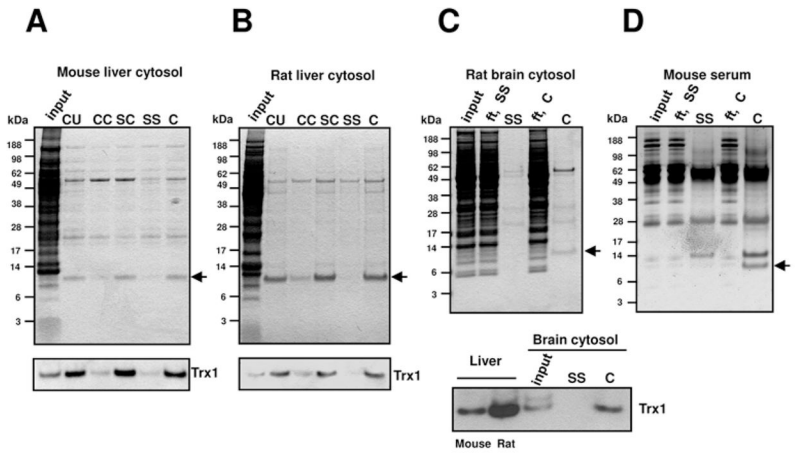

Figure 1. Identification of TR1 targets in cytosolic fractions of mouse and rat tissues

Mouse liver, rat liver, rat brain cytosolic fractions, or mouse serum, were loaded on to the TR1-immobilized resins indicated (designated based on amino acids at the cysteine–selenocysteine positions in the C-terminus of TR1, see text for description). Bound proteins were eluted with DTT and analysed by SDS/PAGE. Coomassie Blue staining was used to visualize proteins. (**A**) Mouse liver cytosol, (**B**) rat liver cytosol and (**C**) rat brain cytosol. Lower panels (**A**–**C**) show Western blotting with anti-Trx1 antibodies (mouse liver and rat liver cytosolic fractions were used as controls for rat brain). (**D**) Mouse serum (silver staining). Molecular mass markers (in kDa) are shown on the left-hand side. Input is an initial cytosolic fraction. ft is a flow-through protein fraction for SS and C resins respectively. Arrows show Trx1 bands. CU, Cys–Sec; CC, Cys–Cys; SC, Ser–Cys; SS, Ser–Ser; C, Cys-truncated mutant.

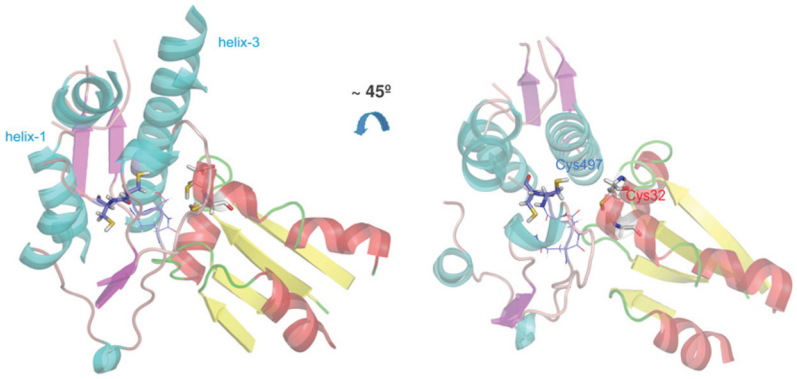

Figure 2. Structural analysis of TR1–Trx1 interaction

Docking of TR1 (in cyan, with violet ribbon representation) with Trx1 (in red and yellow ribbons) is shown. Catalytic cysteine residues (Cys^{32} and Cys^{35} for Trx1, and Cys^{497} and Sec^{498} for TR1) are shown in stick representation. The C-terminal active site of TR1 is shown in blue wire frame (except for the catalytic cysteine residue, depicted in stick representation). The Figure shows the best docking position found (energy score for the complex is −370 kcal/mol) from two different angles (45 °rotation in the direction of the arrow shown). Helices 1 and 3 are labelled. Helix 1 is the first helix in the TR1 structure (spans residues 22–34). Cys^{497} and Sec^{498} are close to helix 3 and helix 1 respectively. In our analysis, the interaction between Trx1 and TR1 occurs on the side of helix 3, bringing Cys^{32} in Trx1 close to Cys^{497}.

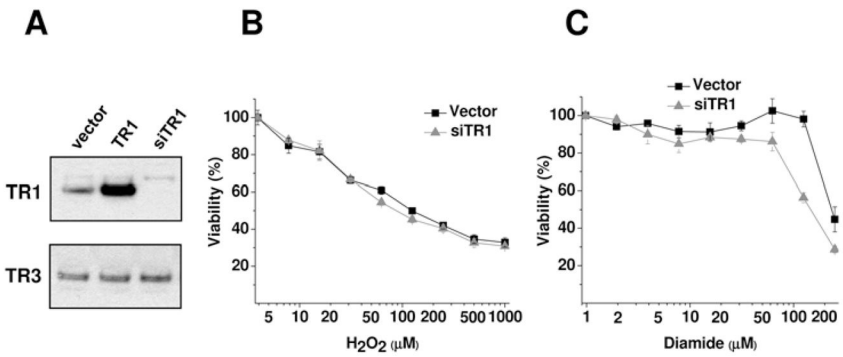

Figure 3. Sensitivity of TR1-knockdown cells to oxidative stress

TCMK-1 cells were stably transfected with pU6 (vector), pU6-TR1 overexpressing construct (TR1) and TR1-knockdown construct siTR1-3 (siTR1). (**A**) Levels of TR1 and TR3 expression in control, TR1-overexpressing and TR1-knockdown cells as assayed by Western blotting. (**B**) TCMK-1 control and TR1-knockdown cells were treated with the indicated concentrations of hydrogen peroxide, cell viability was determined and the results are represented as means ± S.D. of four replicates. (**C**) TCMK-1 control and TR1-knockdown cells were treated with the indicated concentrations of diamide, cell viability was determined and the results are represented as means ± S.D. of four replicates.

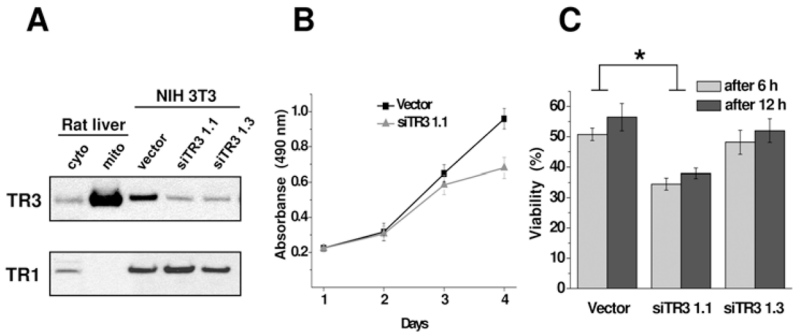

Figure 4. Characterization of TR3-knockdown cells

NIH 3T3 cells were stably transfected with pSec hygro (vector) or the vector encoding two siTR3 constructs, siTR3 1.1 and siTR3 1.3. (**A**) TR3 and TR1 expression in various siTR3 clones and in rat liver cytosolic and mitochondrial fractions assayed by Western blotting with TR1 and TR3 antibodies. (**B**) Growth rate of TR3-knockdown cells. Growth rates of TR3-knockdown (siTR3 1.1) and control (vector) cells were determined and the results are represented as means ± S.D. of four replicates. (**C**) UV treatment of TR3-knockdown cells. TR3-knockdown and control (stably transfected with pSEC hygro) cells, assayed 6 or 12 h after exposure to UV irradiation as described in the Experimental section. * Indicates statistical differences compared with the vector control by using the two-tailed Student's *t* test ($P < 1 \times 10^{-4}$ for 6 h and $P < 0.003$ for 12 h respectively).

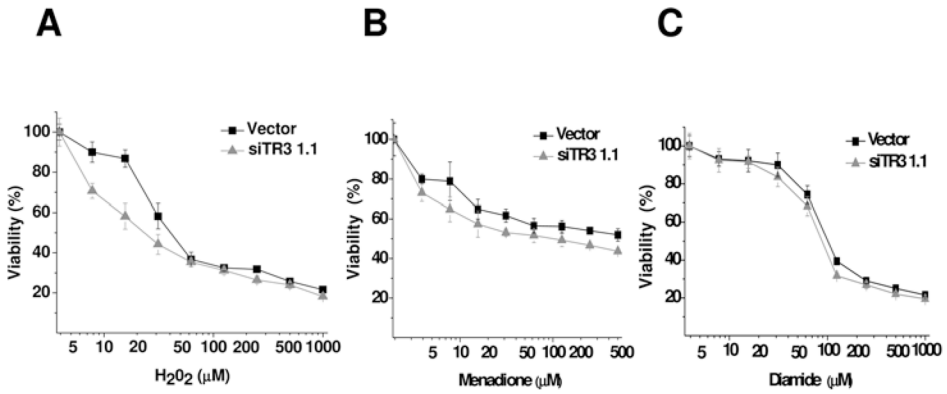

Figure 5. Sensitivity of TR3-knockdown cells to oxidative stress

siTR3 1.1-knockdown cells or cells stably transfected with pSec hygro (vector) were treated with the indicated concentrations of oxidants, cell viability was determined, and the results represented as means ± S.D. of four replicates. (**A**) Treatment with hydrogen peroxide. (**B**) Treatment with menadione. (**C**) Treatment with diamide.

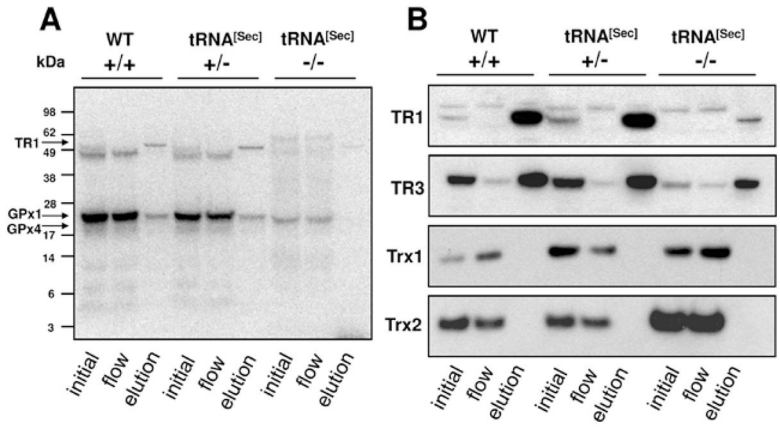

Figure 6. ^{75}Se metabolic labelling and affinity isolation of TRs from mice with liver-specific *Trsp* knockout on ADP–Sepharose

Mice with genotypes *Trspfl/fll-Alb-Cre*+/− (+/−), *Trspfl/+-Alb-Cre*+/− (−/−) and *Trspfl/fll* (WT) were labelled with ^{75}Se. Liver lysates were loaded on to ADP–Sepharose resins, the resins extensively washed with loading buffer and bound proteins eluted with SDS/PAGE loading buffer. Isolated proteins were subjected to SDS/PAGE followed by Western blotting with antibodies specific for TR1, TR3, Trx1 and Trx2. (**A**) ^{75}Se-labelled proteins detected with a PhosphorImager after affinity isolation of TRs. Molecular mass markers (in kDa) are shown on the left-hand side. (**B**) Western blotting analysis of TR1, TR3, Trx1 and Trx2 expression in samples shown in (**A**). Initial, flow and elution indicate initial liver lysates which were loaded on to ADP–Sepharose, flow-through fractions containing unbound proteins and elution fractions enriched for TRs respectively.

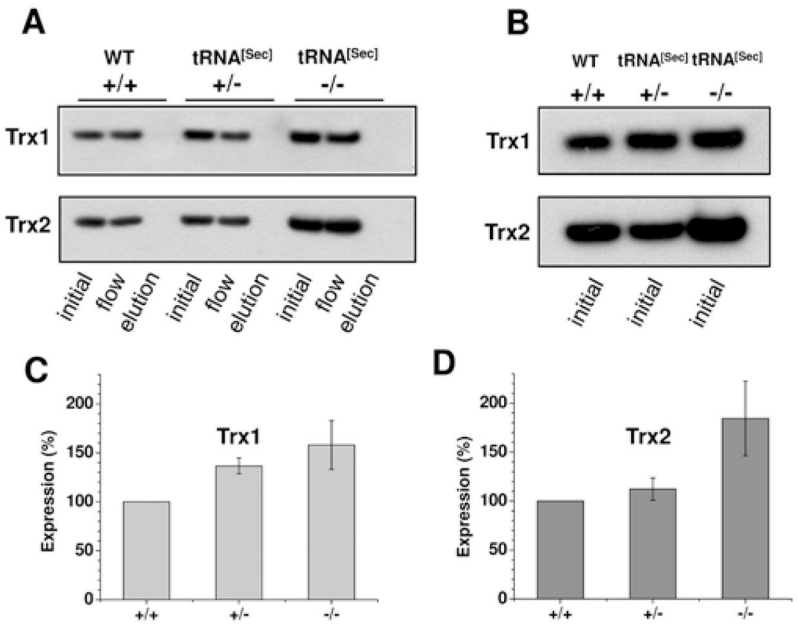

Figure 7. Analysis of Trx expression levels in mice with liver-specific knockout of selenocysteine tRNA

Liver lysates of indicated *trsp* genotypes were subjected to ADP–Sepharose affinity isolation. Isolated proteins were analysed by SDS/PAGE followed by Western blotting with antibodies specific for Trx1 or Trx2. (**A**) Initial, flow-through and elution fractions from ADP–Sepharose were analysed. (**B**) Only the initial liver lysates were analysed. Initial, flow and elution indicate initial liver lysates which were loaded on to ADP–Sepharose, flow-through fractions containing unbound proteins and elution fractions enriched for TRs respectively. (**C** and **D**) Band intensities from the initial fractions for Trx1 and Trx2 correspond to WT, heterozygous and homozygous knockout samples (as shown in **B**, initial) were quantified using ImageQuant. Results are represented as means ± S.D. for three independent experiments in which values for WT samples correspond to 100 %.

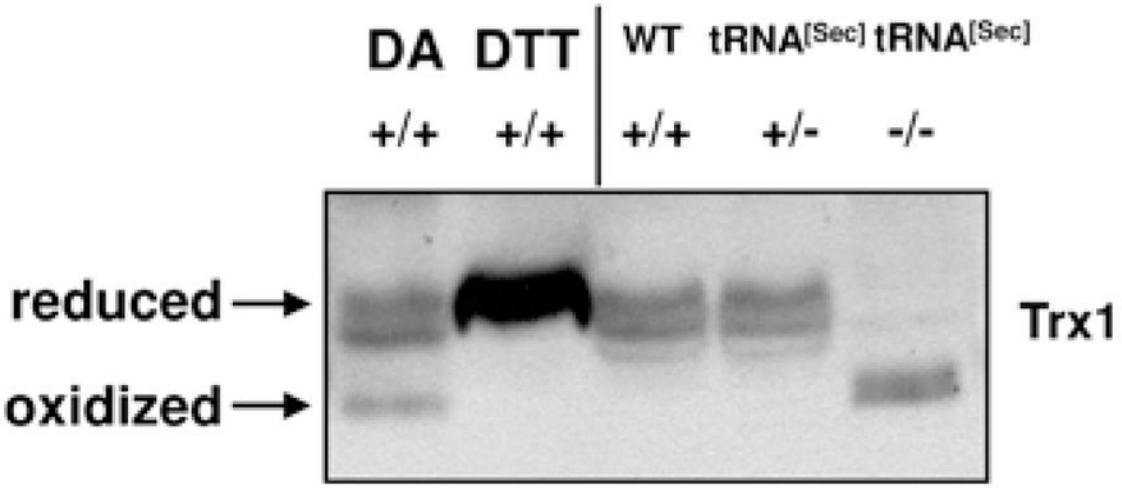

Figure 8. Analysis of the redox state of Trxs in livers of WT and liver-specific selenocysteine tRNA-knockout mice

Liver extracts were treated with AMS, a compound that alkylates cysteine residues resulting in a decreased mobility on gels. Control (WT) samples were incubated with diamide (DA) or with DTT prior to AMS alkylation to generate oxidized and reduced Trx samples respectively (two left-hand lanes). Proteins were subjected to SDS/PAGE followed by Western blot analysis with antibodies specific for Trx1.